

Machinability of high strength molybdenum-refined graphite grey cast iron and conventional vermicular automobile engine heads using heptagonal and double-sided carbide inserts

Alcione dos Reis

Matheus Gonçalves de Ataíde (✉ matheus.ataide@ufu.br)

Universidade Federal de Uberlândia <https://orcid.org/0000-0003-1499-685X>

José Aécio Gomes de Souza

Luiz Leroy Thomé Vaughan

Rhander Viana



Álison Rocha Machado

Research Article

Keywords: automotive industry, machining power, milling, high strength cast iron

Posted Date: October 12th, 2022

DOI: <https://doi.org/10.21203/rs.3.rs-2118414/v1>

License:   This work is licensed under a Creative Commons Attribution 4.0 International License. [Read Full License](#)

Abstract

In the current scenario, industry has been faced with growing restrictions imposed by law, aimed at reducing the emission of fuel gases and pollutants into the atmosphere. The automotive industry is seeking to produce vehicles with higher performance to match these needs, so that engines become increasingly smaller, less pollutant and silent. Regulatory factors have guided and contributed to the development of new technologies applied to the internal combustion engine. Depending on such developments, maximum injection and combustion pressures can be achieved, thus, ensuring more efficiency and better performance, in addition to emission reduction. However, recent technology requires engines to withstand even greater mechanical stresses, which can inevitably lead to a component premature failure if no additional improvement are made. Therefore, there has been an incessant search for an alloy capable of replacing conventional gray cast iron, commonly used in the manufacture of blocks, but not yet suitable for high pressures. This work objective is to evaluate the face milling cutting power behavior in FC300 high strength cast iron with the addition of molybdenum and refined graphite, grade (FC300_{Mo+RG}), for application in engine heads, compared to alloys already used for this purpose, such as the FC250 gray cast iron, the FC300 molybdenum alloyed gray cast iron, grade (FC300_{Mo}), and the FV450 vermicular cast iron, grade (CGI).

1. Introduction

With the growing demand in the metalworking industry, the production of cast irons, that represents much of the market, has greatly increased in recent years. Therefore, the continuous search for improvements in properties has led several industries and university centers to the development of numerous studies in order to remain competitive [Lyu, 2019]. The addition of elements such as silicon, magnesium, chromium, molybdenum and copper, combined with the appropriate heat treatments, has significantly contributed to the improvement of the mechanical properties of cast irons, such as stiffness and ductility [Srivastava et al., 2020], making their use viable in applications previously exclusives to medium carbon content steels [Fengzhang et al., 2009].

New materials are developed to integrate in the most complex and important vehicle systems, such as engines, chassis, suspension and they should provide a degree of engineering performance superior to that found in conventional materials. However, there are numerous issues involved in the development of a new material. In principle, the automotive industry has been prioritizing weight reduction, which depends on technological innovations in several adjacent areas [Guessser et al., 2015]. In this perspective, research and product development ventures have been considered as industrial competitiveness factors, enabling companies achieve greater market margins.

According to Schultheiss et al. [2018] and Masuda et al. [2021], gray cast iron is a widely used material in the manufacture of blocks and heads, gears, brake disks, hydraulic systems, pneumatic equipment, as well as of in combustion engine and industrial machinery. According to Fontaras et al. [2017], despite some energy efficiency research advances, internal combustion engines continue to be one of the largest major cities sources of pollutants worldwide.

Srivastava et al. [2018] state that the increasing gas compression rates of engine blocks have improved the efficiency of automobiles, which ultimately drove the attention to new materials for this application. However, a compression rate increase can cause these components to crack [Polak *et al.*, 2005]. Therefore, the addition of a small amount of alloying elements are mainly necessary to improving materials' strength, which significantly increases the life span of the components [Sun et al., 2020]. According to Shen [2003], the mechanical strength of grey cast iron does not allow higher pressures to be reached in engine blocks. On the other hand, it possesses particularly good thermal conductivity and vibration damping characteristics.

Another class of material employed in the manufacture of these components, especially in diesel engines, is the vermicular cast iron, of which its high mechanical strength, compared to gray cast iron, allows the achievement of higher compression rates, which can result in thickness reductions [Da Silva et al., 2020]. Notwithstanding, its mechanical and physical characteristics are costly, especially in machining processes, due to higher process times and increased tool wear, leading to longer machine downtime and reduced production capacity [Guo et al., 2014].

According to Lu et al. [2020], the difficulty in machining vermicular cast iron is primarily associated with two main factors: its high mechanical strength, that involves large cutting forces, and the absence of manganese sulfide, always present in the microstructure of gray cast irons, which deposits on the cutting tool and ensures a local natural lubrication.

Thus, the material's choice for automotive industry applications should be based on the following characteristics: weight, mechanical strength, material cost, environmental considerations and machining cost [Malakizadi et al., 2018]. According to Agunsoye et al. [2013], to understand the mechanical properties of cast irons, it is necessary to understand the microstructure formation in these materials and how the chemical composition variables, or processing, affect the microstructure. This knowledge usually bares to the manufacturer of the piece, but a broad discussion of some fundamentals and limitations, including how alloying elements influences the machinability, helps the designer in the perception of what is possible to achieve with cast irons [Suhaimi et al., 2017].

Machinability is a variable that deserves special attention and should be analyzed along with the improvement of desired mechanical properties, being its study fundamental towards the selection of metallic materials for various other industrial applications [Trent *et al.*, 2000].

2. Experimental Methodology

It was evaluated the face milling cutting power behavior in FC300 high strength cast iron with the addition of molybdenum and refined graphite, grade (FC300_{Mo+RG}), for application in engine heads, compared to alloys already been used for this purpose, such as the FC250 gray cast iron, the FC300 molybdenum alloyed gray cast iron, grade (FC300_{Mo}), and the FV450 vermicular cast iron, grade (CGI). Two carbide tool geometries were selected for the machining tests. The whole process occurred without the addition of cutting fluids.

The materials used in this work were provided by TUPY S.A, located in Joinville/Brazil. The dimensions of the specimens were 400 mm long, 240 mm wide and 40 mm thick. The chemical composition of the cast bars was carried out by emission spectrometry. During manufacturing, cupped-coin specimen was removed from the liquid metal after nodularization and inoculation treatments, being subsequently poured into a water-cooled copper-coin. Then, it was ground and analyzed in an ARL optical emission spectrometer.

The Brinell hardness values were obtained by a Wolpert durometer and the mechanical strength values by an EMIC tensile machine. To ensure good impression and prevent excessive elastic recovery of the material, the loadings were conducted for 30s on the tested surfaces. Table 1 presents further information regarding the cast irons used.

Table 1
Chemical composition and mechanical properties of the materials

| Materials | Si [%] | Mn [%] | P [%] | S [%] | Cr [%] | Ti [%] | Sn [%] | Cu [%] | Hardness [HB] | Yield strength [MPa] | Ultimate tensile strength [MPa] | Elongation [%] |
|------------------------------------|--------|--------|-------|-------|--------|--------|--------|--------|---------------|----------------------|---------------------------------|----------------|
| FC250 | 1.95 | 0.55 | 0.025 | 0.100 | 0.27 | 0.01 | 0.13 | 0.28 | 187 | – | 259 | – |
| FC300_{Mo} | 2.11 | 0.50 | 0.036 | 0.100 | 0.23 | 0.01 | 0.06 | 0.67 | 207 | – | 278 | – |
| FC300_{Mo} + RG | 2.12 | 0.66 | 0.035 | 0.100 | 0.23 | 0.01 | 0.06 | 0.67 | 217 | – | 283 | – |
| FV450 | 2.21 | 0.32 | 0.019 | 0.003 | 0.03 | 0.01 | 0.07 | 0.99 | 229 | 379 | 524 | 1.54 |

For the development of the two-level factor matrices and determination of the interlamellar perlite spacing, by using a Hitashi scanning electron microscope - model TM3000, the samples were rinsed with 3% Nital reagent. A total of 25 areas were

randomly selected and enlarged in 20000x magnification at different surface regions. For the measurement of the intersections of the cementite lamellae, 25 zones were also selected, using the same methodology adopted by Voort et al., (1984).

The machining tests were performed in a Discovery CNC vertical center - model 760, with main motor power of 11 KW, maximum speed of 10000 RPM, manufactured by ROMI Bridgeport. Two different carbide tool geometries were used, both without coatings, as represented in Fig. 1.

Table 2 shows the specifications of the cutting tools and cutters used. Both the inserts and cutters were manufactured by Walter Tools. During the dry machining tests, two carbide geometries were used (heptagonal insert and double-sided insert) with a variation of the cutting tool speed.

There was performed a 2^k factorial design, where k was equal to 4, as it relates to: cutting speed, cutting feed, workpiece material and cutting type. The qualitative variables as workpiece material and cut type had, respectively, 4 and 2 levels. Table 3 represents the values of the quantitative variables, as well as other cutting parameters. All tests were carried out without applying cutting fluid.

Table 2
Specifications

| | | Geometry A | Geometry B |
|---------------|----------------------------------|-----------------------------------|------------------------------------|
| Insert | Tool format | Heptagonal | Double-sided |
| | Code | XNHF0906ANN-D57-WKP25S Tiger-tec® | LNHU130608R-L55T-WKP25S Tiger-tec® |
| | Number of edges | 14 | 4 |
| | Cutting edge length | 9 mm | 13 mm |
| | Insert thickness | 6.35 mm | 6.80 mm |
| | Tip radius | 0.80 mm | |
| | Straightening edge length | 1.4 mm | 2.2 mm |
| | Class | WKP 25S | |
| Cutter | Model | Xtrac-tec® | BLAXX |
| | Code | F4045.B27.080.Z09.06 | F5141.B27.080.Z10.12 |
| | Diameter | 80 mm | |

Table 3
Cutting parameters

| Tool format | v(m/min) | f _z (mm/dente) | a _e (mm) | a _p (mm) | Tipo de corte | Materials |
|------------------|----------|---------------------------|---------------------|---------------------|---------------|--------------------------|
| A (Heptagonal) | 350/230 | 0.1/0.2 | 60 | 1 | Concordante/ | FC250 |
| | | | | | Discordante | FC300 _{Mo} |
| B (Double-sided) | | | | | | FC300 _{Mo + RG} |
| | | | | | | FV450 |

For the acquisition and monitoring of the cutting power, a current transducer - model HAS 50S, and a voltage transducer - model LV 20-P, were coupled directly on the power supply network of the machine, as well as the operational 741-Series amplifiers and a

data acquisition device from National Instruments with a converter of 16 inputs, containing 16 bits - model NI USB-6221 with acquisition capacity of 250 kS/s, as shown in Figs. 2 and Table 4.

The data was transmitted by serial communication via USB to the computer, subsequently treated and stored in text files by Labview® software.

Table 4
– Description of the measuring panel as related to cutting power

| Symbol | Type |
|--------|---------------------------------------|
| A | Current and voltage output signals |
| B | Electric panel |
| C | Electrical voltage conditioning board |
| D | Signal conditioning board outputs |
| E | Electric current conditioning board |
| F | Electrical voltage sensor |
| G | Bus |
| H | Source: Input 110V; 15V Output |
| I | Connection to the electrical network |

3. Results And Discussions

Figure 3 shows the characterization results of the interlamellar spacing and microhardness of the materials and their relationships. It can be observed that the FC300_{Mo+RG} presented the smallest interlamellar perlite spacing, on average 0.29 µm. Its microhardness, on the other hand, was the highest among all gray cast irons and the lowest relative to the FV450 vermicular cast iron. This is an indication that both materials should present an increase in ultimate tensile strength and abrasiveness.

Table 5 represents the statistical percentage difference of the interlamellar spacings and microhardness average of the materials depicted in Fig. 4. The positive values indicate that there was an increase in the analyzed parameter, while negative values correspond to a reduction. It can be observed that there was no significant statistical difference between the interlamellar spacings of the materials used in this work. On the other hand, the comparisons (FC250 vs FV450), (FC300_{Mo} vs FV450) and (FC300_{Mo+RG} vs FV450) showed a significant statistical difference in microhardness.

Table 5
Statistical percentage difference of interlamellar spacings and microhardness

| Comparison | Interlamellar spacings | | Microhardness | |
|---|------------------------|---------|---------------|---------|
| | Diference | p-value | Diference | p-value |
| FC250 vs FC300 _{Mo} | - 6.06% | 0.4359 | + 4.67% | 0.2873 |
| FC250 vs FC300 _{Mo+RG} | - 12.12% | 0.1912 | + 12.58% | 0.0633 |
| FC250 vs FV450 | - 3.03% | 0.6213 | + 30.93% | 0.0009 |
| FC300 _{Mo} vs FC300 _{Mo+RG} | - 6.45% | 0.5449 | + 16.29% | 0.2339 |
| FC300 _{Mo} vs FV450 | + 3.22% | 0.7081 | + 25.08% | 0.0040 |
| FC300 _{Mo+RG} vs FV450 | + 10.34% | 0.3296 | + 16.29% | 0.0276 |

Figure 4 shows the behavior of the current signal measured throughout the machining of the cast iron material FC250. The current average is used to calculate the cutting power for each test.

Figures 5 and 6 represent the cutting power, derived from the deduction of the power measured during milling, already with the due subtractions of the power acquired in the empty mode. In all, one test and two repetitions were performed for each set of cutting parameters.

It is noted that the cutting power tends to increase with the increase of the cutting speed. This is also accompanied by a higher generation of heat and, consequently, by a reduction of the material strength, which, in turn, further facilitates the machining and dismantling of the material. This is typical of ductile materials like steels, but not so common for brittle materials like cast irons. As for the latter, the chip is discontinuous, so that higher cutting speeds increases the thickness of the lamellae and, consequently, intensifies the force, rather than diminishing it [Trent *et al.*, 2000].

For Gabaldo *et al.*, [2009], cutting power has an important influence on the milling process of cast irons, especially those used in the manufacture of engine blocks. With higher wear on the cutting edges, the contact area between workpiece and tool increase chip deformation. Consequently, the power consumption required to cut cast iron also increases.

Another important factor to be considered in the long run is the machine stability during servicing, which depends on the quality and state of maintenance. It can be seen that the cast iron FV450, Fig. 7, was the only that caused the highest power consumption. This alloy has also the highest ultimate tensile strength and hardness among all studied materials. On the other hand, the graphs show that the material presenting the lowest cutting power was the FC250, followed by the FC300_{Mo}.

Diniz *et al.*, [2006] state that the increase in power is not only linked with flank wear, but also to other types of wear and failures that can, as in the case of crater wear, inversely decrease the power consumption as the effective angle of exit increase.

According to Bagetti *et al.*, [2009], the high strength and hardness of vermicular cast iron promotes higher cutting forces than conventional grey cast irons, thus, requiring about 20–30% more power for simple machining operations, as well as more robust clamping systems.

Tables 6 and 7 represent Figs. 5e 6 as for the average and statistical percentage difference in the shear power. The positive values indicate that there was an increase in cutting power, whereas the negative indicate a reduction.

Table 6
 Statistical percentage difference of the cutting power ($v = 230$ m/min; $f_z = 0.1$ mm/tooth)

| Tool | Comparison | Concordant | | Discordant | |
|----------|---|------------|---------|------------|---------------|
| | | Diference | p-value | Diference | p-value |
| A | FC250 vs FC300 _{Mo} | + 39.85% | 0.0013 | + 1.28% | 0.7699 |
| | FC250 vs FC300 _{Mo + RG} | + 46.50% | 0.0008 | + 18.18% | 0.0152 |
| | FC250 vs FV450 | + 64.12% | 0.0003 | + 40.71% | 0.0012 |
| | FC300 _{Mo} vs FC300 _{Mo + RG} | + 4.75% | 0.3187 | + 16.68% | 0.0197 |
| | FC300 _{Mo} vs FV450 | + 17.35% | 0.0176 | + 38.92% | 0.0014 |
| | FC300 _{Mo + RG} vs FV450 | + 12.02% | 0.0501 | + 19.05% | 0.0132 |
| B | FC250 vs FC300 _{Mo} | + 8.61% | 0.1133 | + 6.67% | 0.1887 |
| | FC250 vs FC300 _{Mo + RG} | + 22.58% | 0.0078 | + 71.63% | 0.0002 |
| | FC250 vs FV450 | + 53.01% | 0.0006 | + 41.05% | 0.0012 |
| | FC300 _{Mo} vs FC300 _{Mo + RG} | + 12.86% | 0.0418 | + 60.89% | 0.0004 |
| | FC300 _{Mo} vs FV450 | + 40.86% | 0.0012 | + 32.21% | 0.0025 |
| | FC300 _{Mo + RG} vs FV450 | + 24.80% | 0.0058 | - 17.82% | 0.0088 |

Table 7
Statistical percentage difference of cutting power ($v = 350$ m/min; $f_z = 0.2$ mm/tooth)

| Tool | Comparison | Concordant | | Discordant | |
|---|---|------------------------------|---------|------------|---------|
| | | Diference | p-value | Diference | p-value |
| A | FC250 vs FC300 _{Mo} | + 24.33% | 0.0062 | + 3.62% | 0.4323 |
| | FC250 vs FC300 _{Mo + RG} | + 30.91% | 0.0029 | + 22.63% | 0.0077 |
| | FC250 vs FV450 | + 76.83% | 0.0002 | + 63.02% | 0.0003 |
| | FC300 _{Mo} vs FC300 _{Mo + RG} | + 5.29% | 0.2751 | + 18.34% | 0.0148 |
| | FC300 _{Mo} vs FV450 | + 42.22% | 0.0011 | + 57.32% | 0.0004 |
| | FC300 _{Mo + RG} vs FV450 | + 35.07% | 0.0019 | + 32.93% | 0.0024 |
| | B | FC250 vs FC300 _{Mo} | - 0.41% | 0.9236 | + 9.47% |
| FC250 vs FC300 _{Mo + RG} | | + 15.31% | 0.0255 | + 23.52% | 0.0068 |
| FC250 vs FV450 | | + 39.21% | 0.0014 | + 38.97% | 0.0014 |
| FC300 _{Mo} vs FC300 _{Mo + RG} | | + 15.79% | 0.0233 | + 12.83% | 0.0420 |
| FC300 _{Mo} vs FV450 | | + 39.79% | 0.0013 | + 26.94% | 0.0045 |
| FC300 _{Mo + RG} vs FV450 | | + 20.72% | 0.0102 | + 12.50% | 0.0451 |

It is observed an increase in cutting power with the increase in mechanical strength for the cast irons tested: FC250, FC300_{Mo}, FC300_{Mo + RG} and FV450. It can also be seen that concordant milling has a greater influence on the cutting power difference, when comparing to the tested cast iron alloys.

Once analyzing the power consumed, it can be seen that the FV450 presents the highest ultimate tensile strength and hardness of all studied materials, consequently, being the toughest to cut. On the other hand, the FC250 presented the lowest cutting power at various conditions, whereas the cast irons FC300_{Mo} and FC300_{Mo + RG} depicted intermediate values.

Not only has the FC250 alloy the lowest ultimate tensile strength but also a graphite morphology that facilitates its machining, when compared to the other studied alloys. Many other variables combined play important roles in the tool's life span. As the tool wears down, discrepancies occur in the machining process, as for instance, cause the temperature to rise along with the cutting force or power and change the surface, worsening the final finish [Naves, 2009].

Table 8 shows the analysis of variance of the cutting parameters with a 95% reliability, as indicated in Table 3. It is observed that the variables tolling type, cutting speed, cutting feed and material type have significantly influenced the process. On the other hand, the variable cutting type did not present any influence on the results at all.

Table 8
Analysis of variance for cutting power

| Univariate Tests of Significance ANOVA for machining time: Sigma-restricted parameterization and effective hypothesis decomposition | | | | | |
|---|----------|-----|----------|----------|----------|
| Effect | SS | DoF | MS | F | p-value |
| Intercept | 17118856 | 1 | 17118856 | 3175.810 | 0.000001 |
| Tooling type | 129362 | 1 | 129362 | 23.999 | 0.000048 |
| Cutting type | 5202 | 1 | 5202 | 0,965 | 0.335330 |
| Cutting speed | 333744 | 1 | 333744 | 61.915 | 0.000001 |
| Cutting feed | 302254 | 1 | 312284 | 59.365 | 0.000001 |
| Material type | 449516 | 3 | 149839 | 27.797 | 0.000001 |
| Standard Error | 134760 | 12 | 5390 | | |

Figure 7 represents the correlations between cutting power and interlamellar spacings at various cutting conditions. Taking into account the graphitic phase stress concentration on the surface of the material and its interactions with the pearlitic matrix, it is evident the overlapping effects of the phenomena on the integrity of the shear in the cutting zone, caused by the presence of this second phase.

4. Conclusions

In view of the results presented and the discussions developed, it can be concluded that:

- The addition of molybdenum and graphite refining in the FC300 cast iron have a direct influence on the mechanical properties, promoting an increase of the tensile strength and of the Vickers micro hardness due to the pearlitic nature of the phase;
- The micro hardness in the FC300_{Mo+RG} pearlitic alloy was the highest compared to the FC250 and FC300_{Mo} alloys, but lower than the FV450 vermicular cast iron;
- At $v = 230$ m/min, tool B decreases the cutting power by roughly 15% as compared to tool A at $v = 350$ m/min. On the other hand, tool B at $v = 230$ m/min decreases the cutting power by roughly 24% as compared to tool A at $v = 350$ m/min;
- For the adopted cutting conditions, the cutting power tends to increase with the increase of the cutting speed in these materials: FC250, FC300_{Mo}, FC300_{Mo+RG} and FV450;
- The double-sided insert presents, on average, a 20% decrease in cutting power, relative to the heptagonal insert;
- The FC250 alloy required the lowest cutting power when compared to the FC300_{Mo}, FC300_{Mo+RG} and FV450 alloys;
- Concordant milling has more influence on the cutting power than the discordant milling

Declarations

The authors did not receive support from any organization for the submitted work and they have no competing interests to declare that are relevant to the content of this article.

All authors have consented to participate and publish this article.

Reis, A. and Machado, A. R. conceived of the presented idea. Sousa, J. A. G., Ataíde, M. G., Vaughan, L. L. T. and Viana, R. discussed the results and contributed to the final manuscript.

References

1. Agunsoye, J. O., Isaac, T. S., Awe, O. I., Onwuegbuzie, A. T., 2013, "Effect of silicon additions on the wear properties of grey cast iron", *J. Miner. Mater. Charact. Eng.*, v 1, p 61–67, DOI: <https://doi.org/10.4236/jmmce.2013.12012>;
2. Da Silva, L. R. R., Souza, F. C. R., Guessser, W. L., Jackson, M. J., Machado, A. R., 2020, "Critical assessment of compacted graphite cast iron machinability in the milling process", *Journal of Manufacturing Processes*, v 56, p 63–74;
3. Fengzhang, R., Fengjun, L., Weiming, L., Zhanhong, M., Baohong, T., 2009, "Effect of inoculating addition on machinability of gray cast iron", *Journal of Rare Earths*, vol 27, N 2, p. 294;
4. Fontaras, G., Zacharof, N. G., Ciuffo, B., 2017, "Fuel consumption and CO₂ emissions from passenger cars in Europe – Laboratory versus real-world emissions", *Progress in Energy and Combustion Science*, v 60, p 97 – 131;
5. Guessser, W., Masiero, I., Cabezas, C., 2015, Thermal Conductivity of Gray Iron and Compacted Graphite Iron Used for Cylinder Heads. *Revista Matéria*, vol. 10, n. 2;
6. Guo, Y., Wang, C. Y., Yuan, H., Zheng, L. J., Song, Y. X., 2014, "Milling Forces of Compacted Graphite Iron (CGI) and Gray Iron (GI)", *Materials Science Forum*, v 800, p 32 – 36;
7. Lu, J., Zhang, Z., Yuan, X., Maa, J., Hu, S., Xue, B., Liao, X., 2020, "Effect of machining parameters on surface roughness for compacted graphite cast iron by analyzing covariance function of Gaussian process regression", *Measurement*, v 157, p 107;
8. Lyu, Y., 2019, Abrasive wear of compacted graphite cast iron with added TiN, *Metallography, Microstructure, and Analysis*, vol 8, p 67–71;
9. Masuda, K., Oguma, N., Ishiguro, M., Sakamoto, Y., Ishihara, S., 2021, Sliding wear life and sliding wear mechanism of gray cast iron AISI NO.35B, *Wear*, vol 474, p 203870, DOI: <https://doi.org/10.1016/j.wear.2021.203870>;
10. Malakizadi, A., Ghasemi, R., Behring, C., Olofsson, J., Jarfors, A. E., Nyborg, L., Krajnik, P., 2018, "Effects of workpiece microstructure, mechanical properties and machining conditions on tool wear when milling compacted graphite iron", *Wear*, v 410, p 190–201;
11. Polak, A., Grzybek, J., 2005, "The mechanism of changes in the surface layer of grey cast iron automotive brake disc", v 8, p 475–479;
12. Schultheiss, F., Bushlya, V., Lenrick, F., Johansson, D., Kristiansson, S., Stahl, J. E., 2018, "Tool wear mechanisms of PCBN tooling during High-Speed Machining of gray cast iron", 8th CIRP Conference on High Performance Cutting, vol 77, p 606-609;
13. Shen, J., 2003, "Study on the cutting character and the materials for cylinder block" Harbin: Harbin Institute of Technology, v 6;
14. Srivastava, D. K., Agarwal, A. K., Datta, A., Maurya, R. K., 2018, "Advances in Internal Combustion Engine Research", Springer;
15. Srivastava, R., Singh, B., Saxena, K. K., 2020, "Influence of S and Mn on mechanical properties and microstructure of grey cast iron: An overview", *Materials Today: Proceedings*, v 26, p 2770 – 2775;
16. Suhaimi, M. A., Park, K. H., Sharif, S., Kim, D. W., Mohruni, A. S., 2017, "Evaluation of cutting force and surface roughness in high-speed milling of compacted graphite iron", *MATEC Web Conf., EDP Sci.*, v 101, p 3016;
17. Sun, B. J., Jiang, C. J., Zong, F. L., 2020, Performance and wear of brazing diamond grinding disc in machining gray cast iron, *Diamond and Related Materials*, vol 106, p 107820;
18. Trent, E. M., Wright, P. K., 2000, "Metal Cutting", Elsevier Science;

Figures

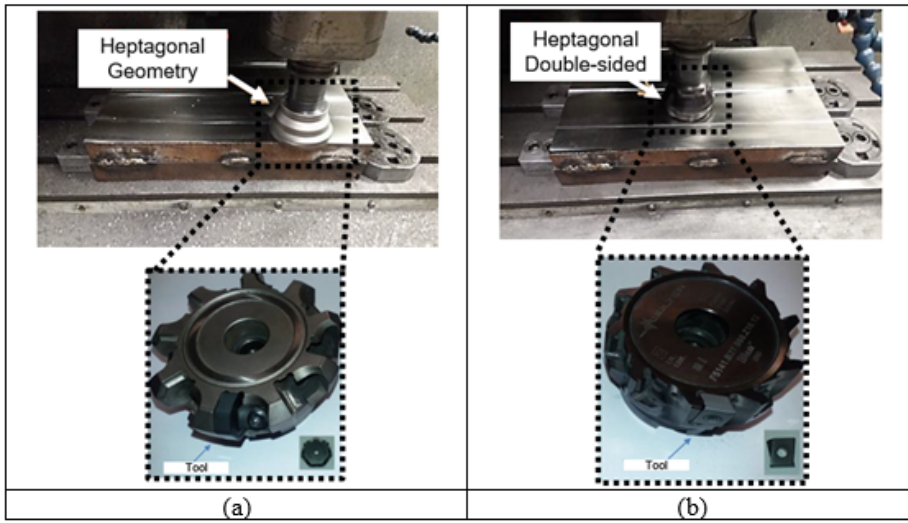


Figure 1

Used tools: (a) Heptagonal; (b) Double-sided

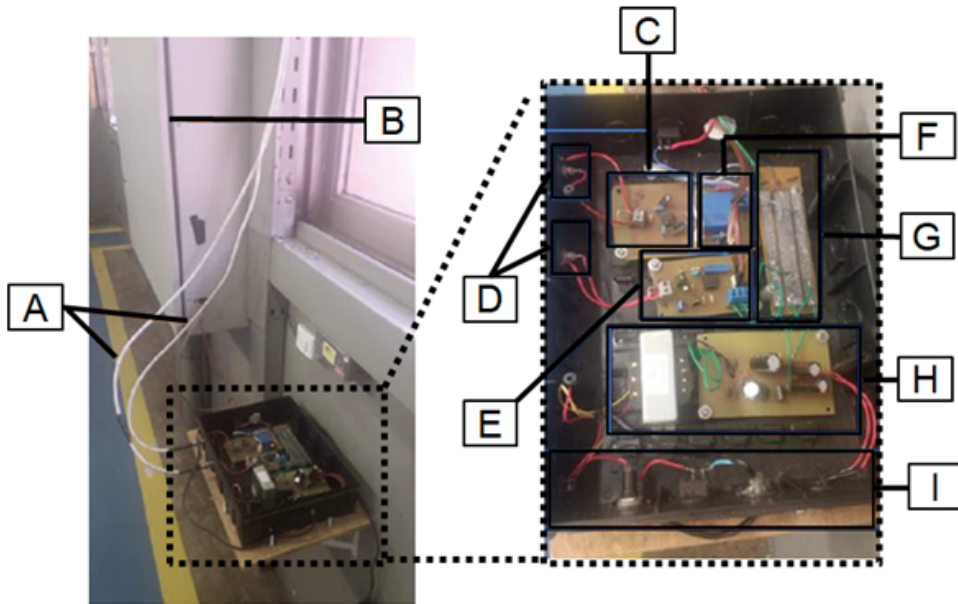


Figure 2

Electrical panel of the cutting machine

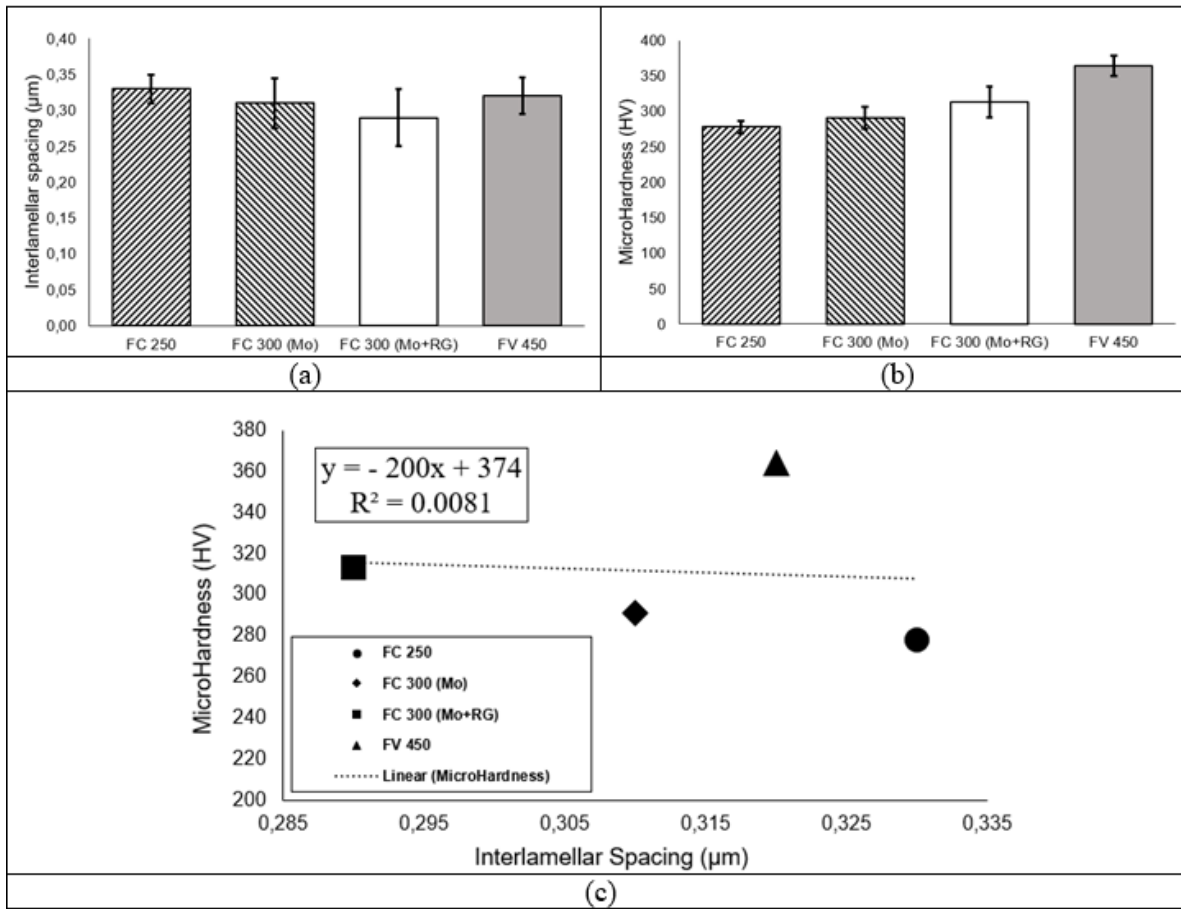


Figure 3

(a) Characterization of perlite interlamellar spacings; (b) Perlite microhardness; (c) Linear regression of microhardness versus interlamellar spacings

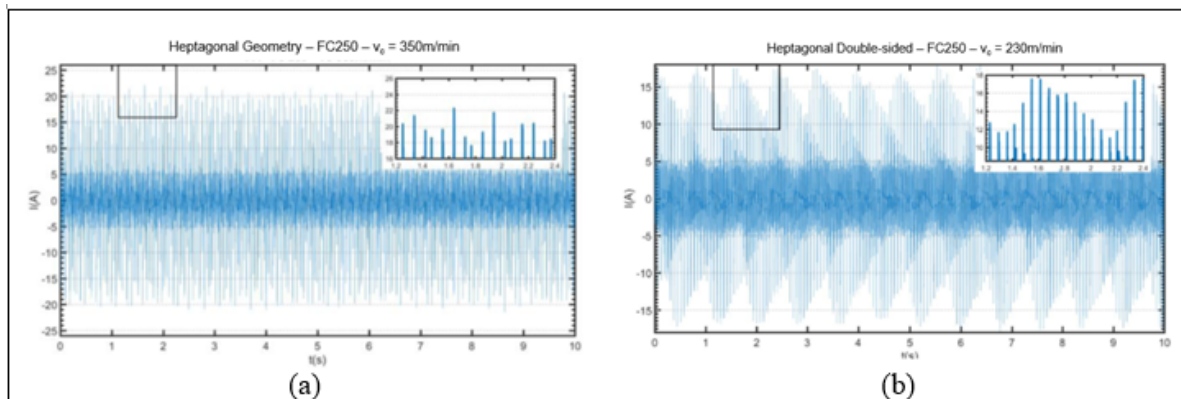


Figure 4

Graphs of the current signal, measured over a pre-test for the FC250 material: (a) Tool geometry A at v = 350 m/min and f_z = 0.2 mm/tooth; (b) Tool geometry B at v = 230 m/min and f_z = 0.1 mm/tooth

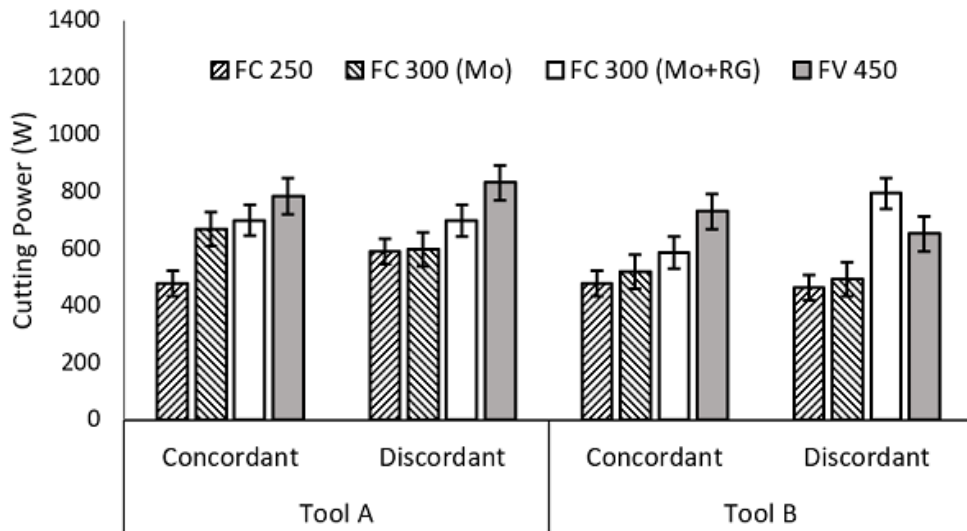


Figure 5

Cutting power during milling ($v = 230$ m/min; $f_z = 0.1$ mm/tooth)

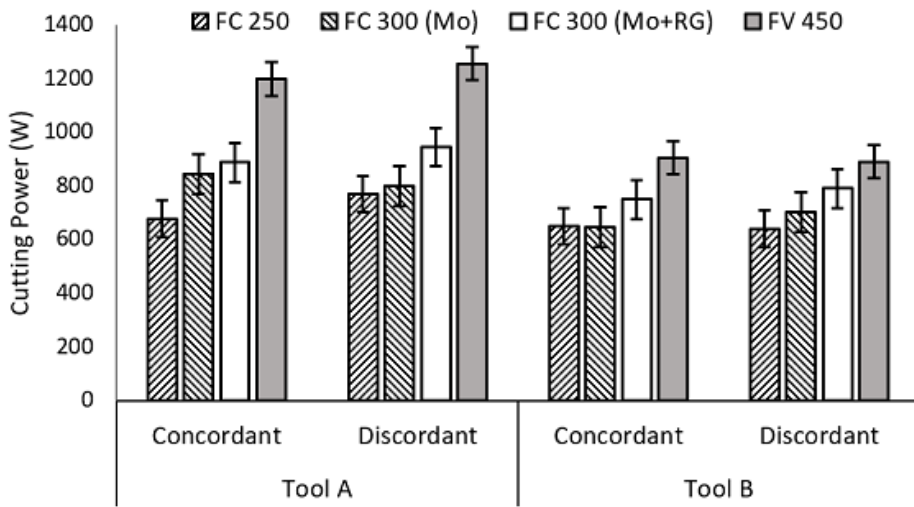


Figure 6

Cutting power during milling ($v = 350$ m/min; $f_z = 0.2$ mm/tooth)

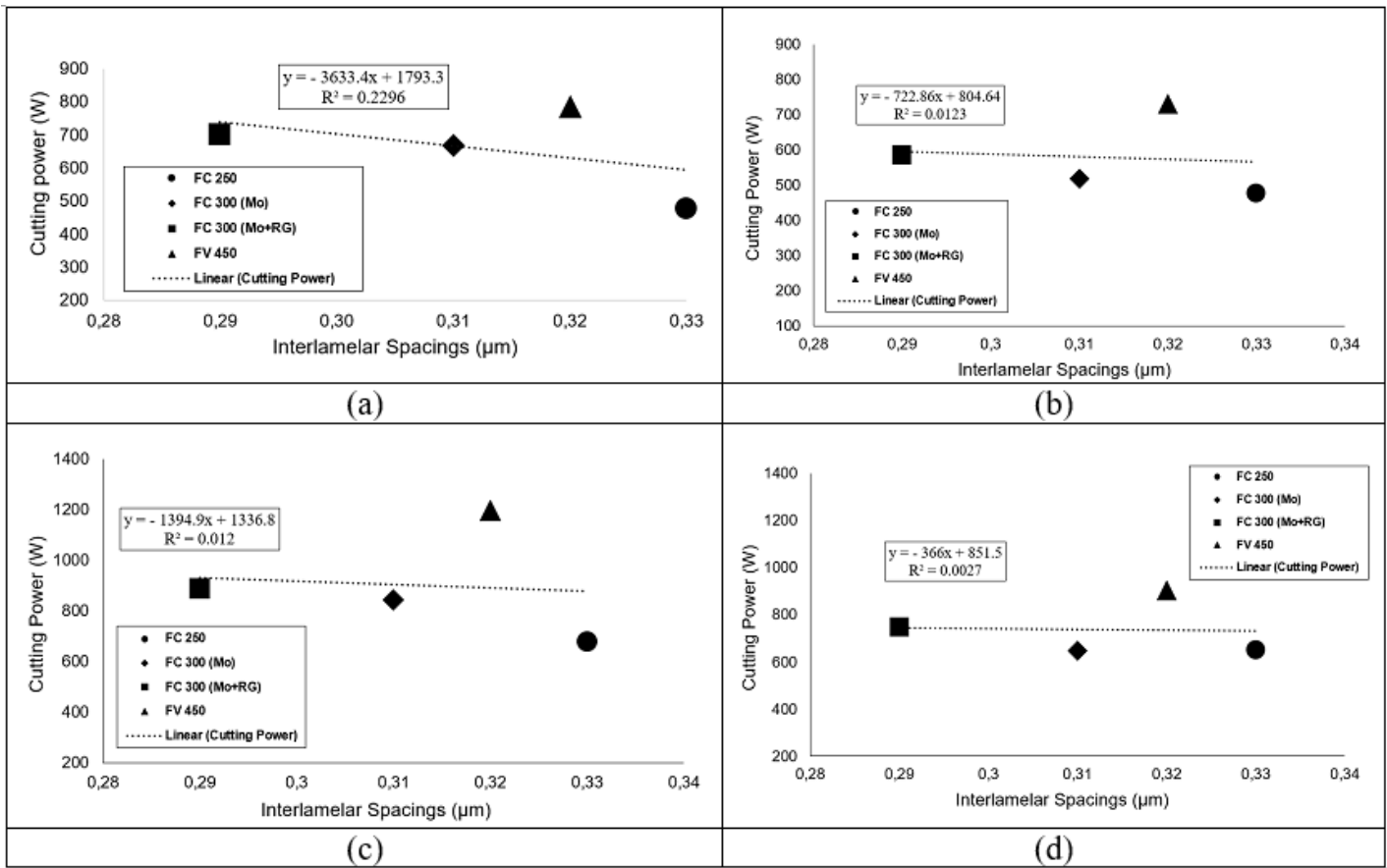


Figure 7

(a) Tool A; $v = 230$ m/min; (b) Tool B; $v = 230$ m/min; (c) Tool A; $v = 350$ m/min; (d) Tool B; $v = 350$ m/min